

Comments on the Refractive Index of Tin Sulphide Nano-crystalline Thin Films

Amit Jakhar, Ashu Jamdagni, Taruna Verma, Vibhav Shukla,
Priyal Jain, Nidhi Sinha and P.Arun

Department of Electronics, S.G.T.B. Khalsa College,
University of Delhi, Delhi 110007, India

&

Ayushi Bakshi

Department of Physics, Hansraj College,
University of Delhi, Delhi 110007, India

August 24, 2018

Abstract

The refractive indices of nano-crystalline thin films of Tin (IV) Sulphide (SnS) were investigated here. The experimental data conformed well with the single oscillator model for refractive indices. Based on the this, we explain the increasing trend of refractive index to the improvement in crystal ordering with increasing grain size.

1 Introduction

Tin Sulphide (SnS) is a semiconducting material with layered structure [1] that has attracted much attention in the past due to its potential application in optical data storage [2] and as an absorbing layer in solar cells [3, 4]. Hence, various techniques have been looked into to fabricate its good quality thin films [5, 6, 7, 8, 9]. While much has been discussed about SnS thin film's band-gap and its strong dependence on fabrication method, relatively less has been done to study the material's refractive index under various conditions. In this manuscript, we discuss the variation of SnS nano-crystalline film's refractive index with grain size.

2 Experimental

Thin films of tin sulphide were deposited using thermal evaporation technique on flat glass substrates. The depositions were carried out at room temperature in a vacuum coating unit (Hind Hi-Vac 12A4D) with vacuum better than 4×10^{-5} Torr. The deposition rate was maintained constant at 2.7 \AA/s . The deposition current and time were controlled to fabricate films of varying thicknesses. A portion of these films were then annealed at two different temperatures, 373 and 473K, for 30 minutes under vacuum of 10^{-3} Torr. Thickness of the films were measured using Dektak surface profiler (150). The influence of film thickness and annealing on the structure of the films were checked using X-ray Diffractometer (Bruker D8 X-ray Diffractometer) operating at the 40 KV and 40 mA with $\text{CuK}\alpha$ radiation ($=1.5406 \text{ \AA}$) and Transmission Electron Microscopy (Technai T30U Twin). The optical absorption and transmission spectra of the films were recorded as a function of wavelength using an UV-Vis Double Beam Spectrophotometer (Systronics 2202) over the range 300-1100 nm with unpolarized light incident normal to the film surface.

3 Results and Discussion

3.1 The Structural and Morphological Analysis

As grown and annealed (at 373 K and 473 K) SnS thin films of different thicknesses (namely 270, 480, 600, 630 and 900 nm) were used in this study. The films were found to be uniform and dark brown in color. There was negligible or no change in the color of the films upon annealing. SnS is known to have a layered structure as mentioned in the introduction. The High Resolution Transmission Electron Microscope (HRTEM) image of a 480 nm thick SnS film shown in fig. 1 clearly shows that the film retains the layered structure of its bulk. The crystallographic structures of the as grown and annealed SnS films were analysed by X-ray Diffraction.

Fig. 2 shows a representative X-ray diffractogram of as grown and annealed SnS films of thickness 480 nm. Without exception, the diffraction patterns exhibits (fig 2) peaks at

$(2\theta)=31.1^\circ$, 38.5° and 43.6° corresponding to the (040), (131) and (200) planes which matched well with the orthorhombic structure reported in ASTM card No. 83-1758. The patterns also show that diffraction peaks become more sharp as the annealing temperature increases, possibly implying that the films become more crystalline on annealing. While improvement in ordering with annealing is evident, we found that there was no variation in structure with annealing. The lattice parameters of the unit cell ('a', 'b', and 'c') were estimated by using the positions of the (040), (200) and (131) XRD peaks. Experimentally obtained values of 'a', 'b' and 'c' of the samples were found to be 4.07 ± 0.002 , 11.36 ± 0.01 and 4.45 ± 0.002 Å respectively. The as grown samples of thicknesses 270 and 480 nm were strained, i.e. their lattice parameter ('a') was slightly different. However, this residual stress relaxed on annealing. Only samples with the same lattice parameters are considered here.

The average grain size of the films were calculated from the Full Width at Half Maxima (FWHM) of the XRD peaks using the Scherrers formula [9, 10, 11]

$$r = \frac{0.9\lambda}{\beta \cos\theta} \quad (1)$$

where 'r' is the grain size, β is the FWHM, θ and λ have their usual meaning. The grain sizes were found to vary from 11 to 25 nm depending on the film thickness and annealing temperature (details of which we have reported elsewhere [12]).

3.2 Optical Analysis

From the above analysis it is clear that the films under investigation thus differed only in grain size. Hence, this presented us the opportunity to study the variation of optical properties of SnS as a function of grain size that too in the nano regime. The optical property of a material is represented by its band gap and its refractive index. We use the standard Tauc method [13] to investigate the band gap of SnS films. Fig. 3 shows a $(\alpha h\nu)^2$ vs $h\nu$ plot for a 480 nm thick film where ' α ' is the absorption coefficient and $h\nu$ the photon energy. The band gap of the film was estimated by extrapolating the linear part of the plot to the $h\nu$ axis.

The variation in the band gap with grain size of the films is shown in fig. 4. The trend in variation fits to

$$E = E_g(bulk) + \frac{A}{r^2} \quad (2)$$

where $E_g(bulk)$ is the band gap of SnS in bulk and 'A' a constant relating to the effective mass of the charge carriers in SnS. This result is consistent with properties induced by quantum confinement of electrons [14]. Again this result confirms that SnS grains of 11-25 nm are in the nano-regime.

Many studies investigating the dependence of refractive index on the thickness [15, 16], annealing temperature [17] and substrate temperature [18] have been reported in the literature but no work on its dependence on grain size has been reported so far. Thus, it will be fruitful

to investigate the grain size dependence of the refractive index of the films. The transmission spectra of the films exhibit interference fringes within the wavelength range 300-1100 nm.

The envelope shown in the fig. 5 were drawn connecting the maximas and minimas of the interference peaks. Such envelopes were used to estimate the refractive index of the films using Swanepoels method [19]. Swanepoel method gives the refractive index in the transparent and near band edge region as

$$n = \sqrt{N_1 + \sqrt{(N_1^2 - s^2)}} \quad (3)$$

where

$$N_1 = \frac{2s}{T_m} + \frac{s^2 + 1}{2} \quad (4)$$

and T_m is the minimas of the interference fringes and ‘s’ is the refractive index of the glass substrate. The values of the refractive index (1.5-2.2) are well with in the range found in the literature [20]. Evaluated results show a decrease in the refractive index ‘n’ with increasing wavelength due to the normal dispersion behavior of SnS [21]. Also, the values of the refractive index of the films deposited at room temperature were found to be less than those annealed at 373 and 473 K.

We believe this is a result of improving grain size with annealing. The variation of the refractive index with the grain size is shown in fig. 6. The refractive index ‘n’ of the films follows an increasing trend with the grain size. A pertinent question is why would the refractive index increase with the grain size? To investigate into this question we fit our data to Wemple and DiDomenico (WDD) model [22, 23]. Based on the idea that refractive index of the materials in visible region is due to electron oscillation excitation between conduction and valence band (inter-band transitions in and around the band edge), the refractive index is given as:

$$n^2 = 1 + \frac{E_o E_d}{E_o^2 + (h\nu)^2} \quad (5)$$

where ‘ $h\nu$ ’ is the photon energy, E_o is the single oscillator energy and E_d is the dispersion energy. The dispersion energy, E_d , is the strength of transition and gives the strength of the oscillator. These parameters are derived by fitting a linear function in $(n^2 - 1)^{-1}$ against $(h\nu)^2$ plot. Fig. 7 shows a representative plot of $(n^2 - 1)^{-1}$ against $(h\nu)^2$ of a 480 nm film annealed at 373 K. The intercept (c) and slope (m) of the best fit line to the experimental data give the value of E_o ($= \sqrt{c/m}$) and E_d ($= 1/\sqrt{mc}$).

Fig. 8 shows the variation of E_o and E_d with increasing grain size. While E_o decreases with grain size, E_d increases linearly with grain size. E_d is given as

$$E_d = \beta N_c N_e Z_a \quad (6)$$

where β is the a constant whose value depends on the chemical bonding character of the material, N_c is the co-ordination number, N_e is the total number of valence electrons per anion and Z_a is the chemical valency of the anion. Literature gives the values of β, N_c, N_e, Z_a

as 0.39 eV, 3, 10 and 2 respectively [24]. Considering the samples are identical (barring for change in grain size) with no changes taking place in the crystal structure, one expects E_d to remain constant. However, changes in E_d have been reported before and explained due to increased ordering [15]. Our samples have exhibited improvement in crystalline nature and increased grain size on annealing, as indicated from the XRD plots. Hence, the trend in E_d with grain size is understood.

The observed decrease in the E_o with increasing anneal temperatures can be attributed to quantum confinement in the films. As mentioned, E_o is the single oscillator energy related to the materials band gap. We hence, plot E_o with respect to E_g (figure 9). We find E_o is directly proportional to E_g ($\approx 1.91E_g$). This is consistent with results reported in literature [15]. It is hence natural that the variation of E_o with the grain size is identical to that of the optical band gap (see figure 6).

4 Conclusions

Thin nano-crystalline films of SnS were fabricated on glass substrates kept at room temperature. These films were also annealed. Samples having the same crystalline structure (namely identical lattice parameters) were selected for comparing their refractive indices. Study showed that the film's refractive index is explainable using the single oscillator model and is directly proportional to grain size.

Acknowledgments

This work was supported by University of Delhi under its "Innovation Projects" program (SGTB-101). The authors also acknowledge the assistance rendered by Dr. Binay Kumar, Department of Physics and Astrophysics, University of Delhi.

References

- [1] Ehm L., Knorr K., Dera P., Krimmel A., Bouvier P., Cichy B., Psuja P., Mezouar M., J. Phys.: Condens. Mater. **16**, (2004) 3545.
- [2] Yue G.H., Wang W., Wang L.S., Wang X., Yan X., Chen Y., Peng D.L., J. Alloys Compd. **474**, (2009) 445.
- [3] Gao C., Shen H., Sun L., Shen Z., Mater Lett., **65**, (2011), 1413.
- [4] Noguchi H., Setiyadi A., Tanamura M., Nagatomo T., Omoto O., Sol. Energ Mat Sol C, **35**, (1994), 325.
- [5] El-Nahass M. M., Zeyada H.M, Aziz M.S., El-Ghamaz N.A., Opt. Mat., **20** (2002), 159.

- [6] Hartman K., Johnson J.L., Bertoni M.I., Recht D., Aziz M.J., Scarpulla M.A., Buonassisi T., *Thin Solid Films*, **519**, (2011), 7421.
- [7] Thangaraju B., Kallannan P., *J. Phys. D: Appl. Phys.*, **33**, (2000), 1054.
- [8] Gao C., Shen H., Sun L., *Appl. Surf. Sci.*, **257**, (2011), 6750.
- [9] Yue G.H., Peng D.L., Yan P.X., Wang L.S., Wang W., Luo X.H., *J. Alloys Compd*, **468**, (2009), 254.
- [10] Devika M., Reddy N.K., Reddy D.S., Reddy S.V., Ramesh K., Gopal E.S.R, Gunasekhar K.R., Ganesan V., Hahn Y.B., *J. Phys.:Condens. Matter*, **19**, (2007), 1.
- [11] Cullity B.D. and Stock S.R., “Elements Of X-Ray Diffraction”, 3rd ed. (Prentice-Hall Inc, NJ, 2001).
- [12] Jain P., Arun P., communicated.
- [13] Sajeesh T.H., Jinesh K.B., Kartha C.S., Vijaykumar K.P., *Appld. Surf. Sci.*, **258** (2012), 6870.
- [14] Brus L.E., *J. Chem. Phys.*, **80**, (1984), 4403.
- [15] Selim M.S., Gouda M.E., El-Shaarawy M.G., Salem A.M., El-Ghany W.A.A., *J. Appl. Res.*, **7**, (2011), 955.
- [16] Nwofe P.A., Reddy K.T.R., Tan J.K., Forbes I., Miles R.W., *Phys. Proceedia*, **25**, (2012), 150.
- [17] Devika M., Reddy N.K., Ramesh K., Gunasekhar K.R., Gopal E.S.R., Reddy K.T.R., *Semicond. Sci. Tech.*, **21**, (2006), 1125.
- [18] Ahmed S.M., Latif L.A., Salim A.KH., *J. Basrah Researches (Sciences)*, **37**, (2011), 1.
- [19] Shaaban E.R., Yahia I.S., El-Metwally E.G., *Acta Phys. Pol. A.*, **121**, (2012), 628.
- [20] Turan E., Kul M., Aybek A.S., Zor M., *J. Phys.D: Appl. Phys.*, **42**, (2009), 1.
- [21] Cifuentes C., Botero M., Romero E., Calderon C., Gordillo G., *Braz. J. Phys*, **36**, (2006), 1046.
- [22] Wemple S.H., *Phys Rev. B*, **7**, (1973), 3767.
- [23] Wemple S.H., DiDomenico M., *Phys Rev. B*, **3**, (1971), 1338.
- [24] Safak H., Merdan M., Yuksel O.F., *Turk J. Phys.*, **26**, (2002), 341.

Figure Captions

1. Parallel (040) planes are clearly seen in HRTEM image.
2. X-ray diffraction pattern of a 480 nm thick SnS (a) as grown film. Pattern (b) and (c) are those of same film after annealing at 373 K and 473 K respectively.
3. Plot shows the variation of $(\alpha h\nu)^2$ with photon energy ($h\nu$). The linear region when extrapolated on to the 'X'-axis gives the "allowed-direct transition" optical band-gap.
4. Variation of band-gap with grain size.
5. The transmission spectra of a SnS thin film with envelopes used to calculate the film's refractive index.
6. Variation of refractive index with grain size for two different wavelengths.
7. Representative plot used to estimate E_o and E_d .
8. Variation of E_o and E_d , parameters related to the Wemple and DiDomenico's single oscillator model, shown with grain size. While E_o follows the same trend as the material's band-gap, E_d increases with increasing grain size.
9. Variation of E_o with E_g .

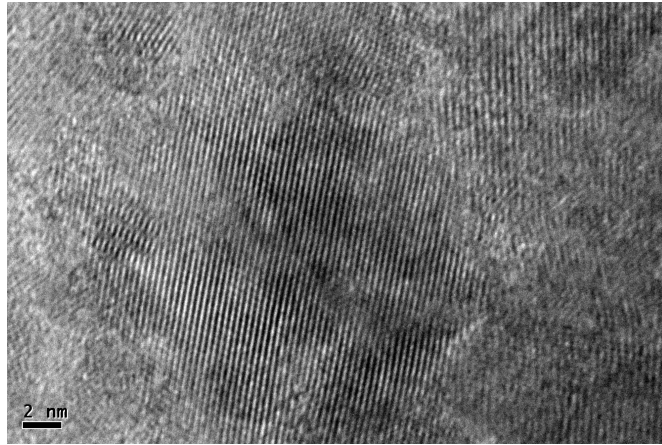


Figure 1: Parallel (040) planes are clearly seen in HRTEM image.

Figures

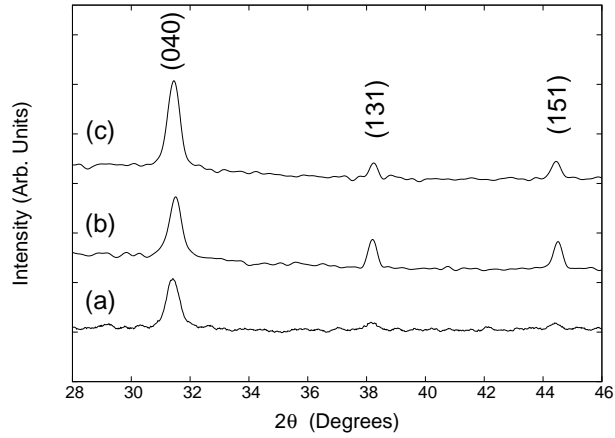


Figure 2: X-ray diffraction pattern of a 480 nm thick SnS (a) as grown film. Pattern (b) and (c) are those of same film after annealing at 373 K and 473 K respectively.

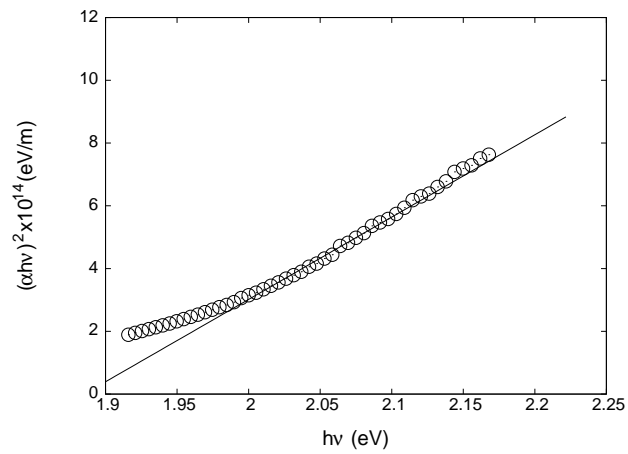


Figure 3: Plot shows the variation of $(\alpha h\nu)^2$ with photon energy ($h\nu$). The linear region when extrapolated on to the 'X'-axis gives the "allowed-direct transition" optical band-gap.

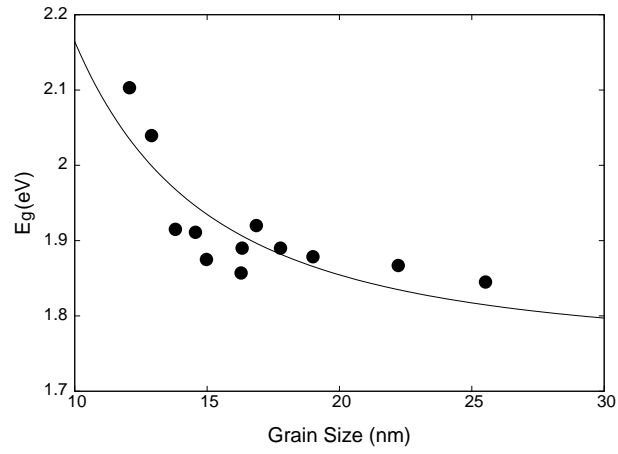


Figure 4: Variation of band-gap with grain size.

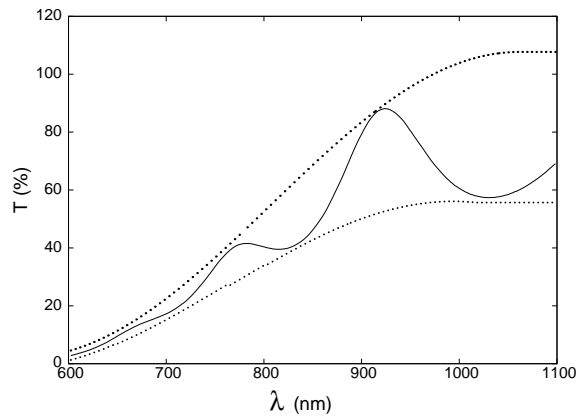


Figure 5: The transmission spectra of a SnS thin film with envelopes used to calculate the film's refractive index.

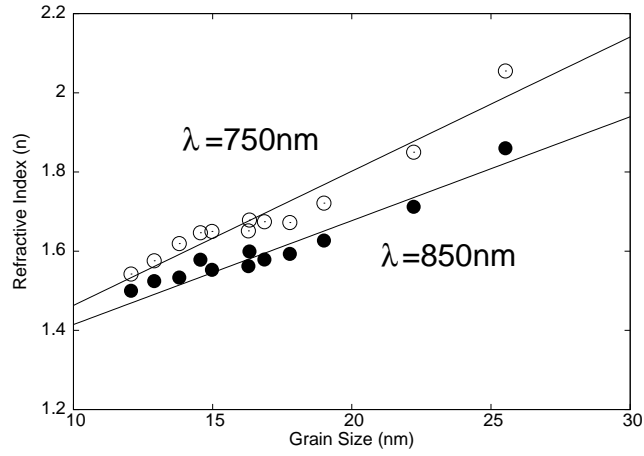


Figure 6: Variation of refractive index with grain size for two different wavelengths.

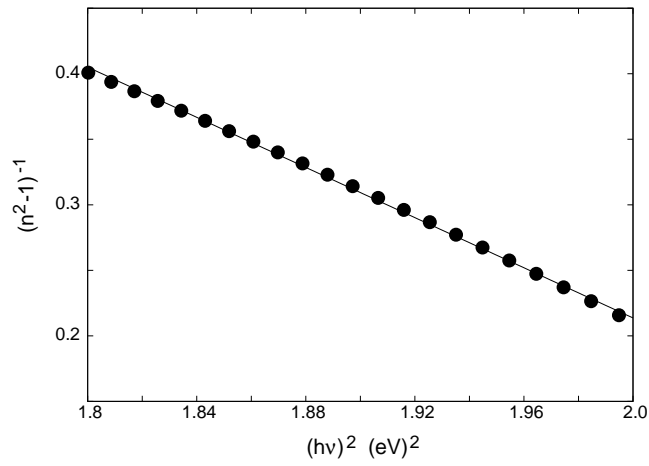


Figure 7: Representative plot used to estimate E_o and E_d .

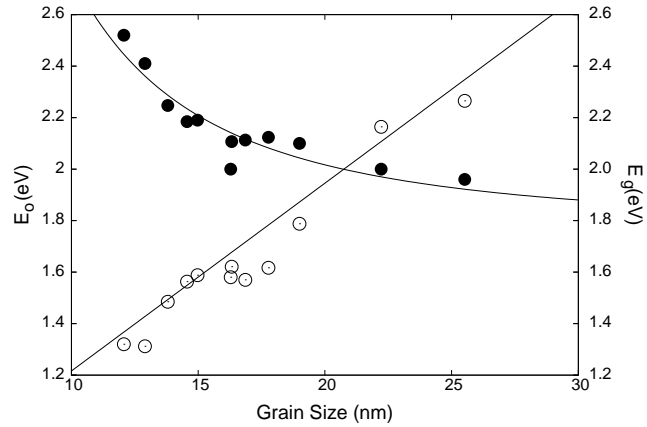


Figure 8: Variation of E_o and E_d , parameters related to the Wemple and DiDomenico's single oscillator model, shown with grain size. While E_o follows the same trend as the material's band-gap, E_d increases with increasing grain size.

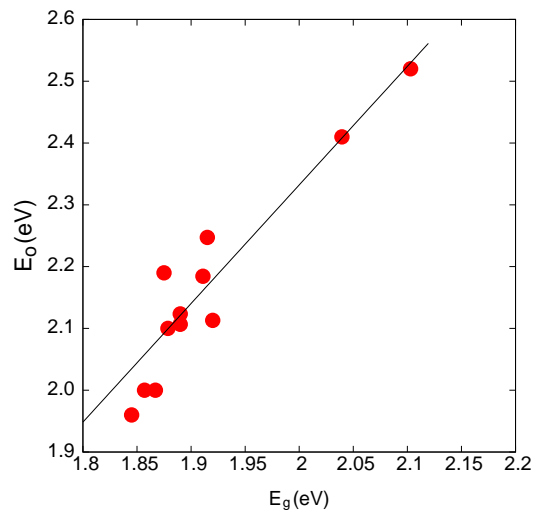


Figure 9: Variation of E_o with E_g .